



Lunar Laser Ranging: a tool for general relativity, lunar geophysics and Earth science

Jürgen Müller¹ · Thomas W. Murphy Jr.² · Ulrich Schreiber³ · Peter J. Shelus⁴ · Jean-Marie Torre⁵ · James G. Williams⁶ · Dale H. Boggs⁶ · Sebastien Bouquillon^{7,8,9,10} · Adrien Bourgoin^{7,11} · Franz Hofmann¹

Received: 27 February 2018 / Accepted: 4 September 2019 / Published online: 17 September 2019
© Springer-Verlag GmbH Germany, part of Springer Nature 2019

Abstract

Only a few sites on Earth are technically equipped to carry out Lunar Laser Ranging (LLR) to retroreflector arrays on the surface of the Moon. Despite the weak signal, they have successfully provided LLR range data for about 49 years, generating about 26,000 normal points. Recent system upgrades and new observatories have made millimeter-level range accuracy achievable. Based on appropriate modeling and sophisticated data analysis, LLR is able to determine many parameters associated with Earth–Moon dynamics, involving the lunar ephemeris, lunar physics, the Moon’s interior, reference frames and Earth orientation parameters. LLR has also become one of the strongest tools for testing Einstein’s theory of general relativity in the solar system. By extending the standard solution, it is possible to solve for parameters related to gravitational physics, like the temporal variation of the gravitational constant, metric parameters as well as the strong equivalence principle, preferred-frame effects and standard-model extensions. This paper provides a review about LLR measurement and analysis. After a short historical overview, we describe the key findings of LLR, the apparatus and technologies involved, the requisite modeling techniques, some recent results and future prospects on all fronts. We expect continued improvements in LLR, maintaining its lead in contributing to science.

Keywords Lunar Laser Ranging · Gravitational physics · Lunar physics · Reference frames

1 Introduction

This paper gives a review of the Lunar Laser Ranging (LLR) technique and analysis. LLR has provided high-precision measurements of the Earth–Moon distance since 1969. Using reflectors placed on the lunar surface by American astronauts and Soviet rovers, LLR involves measuring the round-trip travel time of short pulses of laser light directed to one

reflector at a time. Range precision has improved from a few decimeters to a few millimeters over the decades, constituting a relative raw measurement precision of 10^{-9} – 10^{-11} . Leveraging the raw measurement across the Earth–Sun distance provides another two orders of magnitude for measuring relativistic effects in the Earth–Moon–Sun system.

✉ Jürgen Müller
mueller@ife.uni-hannover.de

¹ Institute of Geodesy, Leibniz Universität Hannover, Hannover, Germany

² Center for Astrophysics and Space Sciences, UC San Diego, La Jolla, CA, USA

³ Geodetic Observatory Wettzell, Technische Universität München, Wettzell, Germany

⁴ Center for Space Research and McDonald Observatory, University of Texas at Austin, Austin, TX, USA

⁵ Observatoire de la Côte d’Azur, Géoazur, Université de Nice Sophia-Antipolis, Caussols, France

⁶ Jet Propulsion Laboratory, California Institute of Technology, Pasadena, CA, USA

⁷ POLAC, SYRTE Laboratory, Observatoire de Paris, Paris, France

⁸ PSL Research University, Paris, France

⁹ CNRS, Sorbonne University, Paris, France

¹⁰ UPMC University, Paris, France

¹¹ Dipartimento di Ingegneria Industriale, University of Bologna, Forlì, Italy

Having the longest observation time series of all space geodetic techniques, LLR allows the determination of a variety of parameters of interest covering Earth–Moon dynamics (e.g., orbit and libration parameters, mass of the Earth–Moon system, cf. Williams et al. 2013; Pavlov et al. 2016; Viswanathan et al. 2018), ephemeris (Folkner et al. 2014; Pitjeva and Pavlov 2017; Viswanathan et al. 2018), lunar physics (Williams et al. 2006; Williams 2007; Williams and Boggs 2015; Pavlov et al. 2016), reference frames and coordinates (e.g., ranging station and lunar reflector coordinates, Müller et al. 2009; Williams et al. 2013; Pavlov et al. 2016; Hofmann et al. 2018) and relativistic physics (e.g., strong equivalence principle, variation of the gravitational constant, metric or preferred-frame effects, Müller 2008; Müller et al. 2008a; Soffel et al. 2008; Williams et al. 2006; Hofmann and Müller 2018). Besides, LLR is also sensitive to nutation/precession, Earth rotation UT0 and polar motion/variation of latitude (cf. Biskupek and Müller 2009a, b; Müller et al. 2015).

2 History

From the earliest of times, observing the Moon has been an interesting and important scientific discipline. Very early observations using parallax achieved an error in the Earth–Moon distance on the order of several thousands of kilometers, which was considered good. When the first spacecraft was sent to the Moon, the uncertainty was kilometers. Today, using laser ranging, the mean distance to the center of mass is known to well less than 1 m and the mean distance to the retroreflectors is known to millimeters: improvements in many orders of magnitude.

Lunar Laser Ranging (Bender et al. 1973) became possible after a retroreflector package was placed on the Moon by the crew of Apollo 11. On August 1, 1969, just 11 days after the placement of the reflector, the first data were obtained by the Lick Observatory (USA: Faller et al. 1969). Later, other observations were made by the US Air Force Cambridge Research Laboratories located in the Catalina Mountains (USA: AFCRL 1969), by the McDonald Observatory (USA), by the Pic du Midi (France) and in Crimea, then in Japan (Kozai 1972), Hawaii and Australia.

Other reflectors have since been landed on the Moon. The second was carried on the Lunokhod 1 rover in 1970 by the Luna 17 mission. In 1971, two more reflectors were landed by the Apollo 14 and Apollo 15 missions (Chang et al. 1972). The last reflector on the Lunokhod 2 rover was put in place in 1973 by the Luna 21 mission.

The observatory for the original Apollo Lunar Ranging Experiment (LURE) was initially to be placed atop Mount Haleakala, on the island of Maui, Hawaii. However, problems at the Haleakala site prevented the facility from being ready for the planned landing in August 1969. A new NASA-funded

telescope had just been completed at McDonald Observatory for planetary observations. The Director, Harlan J. Smith, proposed making the Texas facility available for LURE. Even though preparation could only be begun in the spring of 1969, the facility was made ready and the 2.7-m system became the premiere site for LLR observations through the mid-1980s (Silverberg 1974). McDonald Observatory became the first station to routinely produce observations. The problems at the Haleakala station were eventually solved, and ranges were obtained from 1984 to 1990.

The MLRS (originally Mobile Lunar Ranging Station), designed to be a mobile LLR station for measuring tectonic plate activity on the Earth, was re-configured to be a fixed-location replacement for the 2.7-m McDonald LLR system, also capable of ranging to artificial satellites. The renamed station, McDonald Laser Ranging Station (MLRS: Shelus 1985, 1987), initially placed in the saddle between Mt. Locke and Mt. Fowlkes, became operational in 1983. Wind tunneling effects in the saddle site produced serious problems with atmospheric seeing, and the station was moved to its current position on top of Mt. Fowlkes in early 1988. With the loss in late 2013 (due to age) of the two very high sensitive Varian photomultiplier tubes that served through the 2.7-m as well as the MLRS eras, and not having a suitable replacement, the MLRS is no longer LLR capable. However, Satellite Laser Ranging (SLR) observations continue to the present day.

In parallel, lunar tracking has been developed in France. In 1967, the idea of combining a telescope with a powerful laser was gaining ground. The director of Pic du Midi, Jean Rösch, whose offices were in the former Jolimont Observatory, suggested using the 1.1-m telescope while Alain Orszag from Ecole Polytechnique's laboratory examined the new possibilities opened up by a powerful laser. A ruby laser had been set on the telescope in the Pic du Midi Observatory. This telescope was used both to emit light and to receive it. The first echoes from Lunokhod 1 were obtained on December 1970 (Orszag et al. 1972). Due to some technical problems, these laser emissions were discontinued at Pic du Midi but the decision was taken to build an instrument dedicated to LLR and to install it in the CERGA center for geodynamic and astronomic studies (Veillet et al. 1993) since merged with the Nice Observatory to form the Observatoire de la Côte d'Azur (OCA) near Grasse. The resulting Lunar Laser Ranging station, using a 1.54-m telescope, was a major experiment setup on the Calern plateau, situated in the mountains to the north of Cannes at an altitude of 1270 m. After important modifications (2004–2008), this station was renamed MeO (Metrology and Optics). The new configuration permits both laser ranging (LLR and low- and high-altitude Satellite Laser Ranging) as well as time transfer research (Samain et al. 2008).

For the first 35 years, the majority of LLR measurements were obtained by three stations, see also Fig. 1: McDon-

ald (USA: Shelus et al. 1993), Grasse (France: Veillet 1987; Veillet et al. 1993) and Hawaii (USA). Today new stations are appearing, such as Wettzell (Germany: Schreiber et al. 1992), Matera (Italy), Apache Point Observatory Lunar Laser Ranging Operation (APOLLO) (USA: Murphy et al. 2006, 2008b) and Kunming (China), and projects are in the works in China (Shanghai and Changchun), in Russia (Grechukhin et al. 2016; Vasilyev et al. 2016) and in South Africa (Combrinck 2011).

A revival of interest in LLR has been provided by the opening of the APOLLO Station, which furnishes data of unequaled accuracy (Murphy et al. 2008a). This station is better able to range at full Moon. In 2010, it ranged the reflector emplaced by Lunokhod 1, which lacked a precise position and was unavailable to LLR for four decades until the rover was located on Lunar Reconnaissance Orbiter images (Murphy et al. 2011).

3 Measurement system and observations

3.1 Technique and challenges

LLR relies on a total of five passive reflectors left on the surface of the Moon roughly 49 years ago. The Apollo arrays—landed by the Apollo 11, Apollo 14 and Apollo 15 missions—consist of, respectively, 100, 100 and 300 corner cube reflectors 3.8 cm in diameter operating via total internal reflection, respectively. The Luna 17 and Luna 21 Soviet missions to the Moon landed the Lunokhod 1 and Lunokhod 2 rovers, each carrying identical reflector arrays designed by the French. These arrays consist of 14 triangular-faced corner cubes having edge lengths of 11 cm and silvered rear surfaces. The nominal response of the Lunokhod arrays falls between that of the 100-element and 300-element Apollo arrays.

LLR shares many techniques with SLR, in that short pulses of laser light are directed to a retroreflector target where they bounce back to the station, measuring the departure and arrival times of the pulse to high precision. But the laser link budget for lunar ranging is very marginal due to the overall signal loss, mostly because of the large distance. Beam divergence on both the up leg and down leg results in a signal strength that depends on the inverse-fourth power of distance. This results in the lunar return signal being 10^7 times weaker than that from a similar reflector at the distance of the LAGEOS satellite, for instance. Thus, even today, only very few terrestrial stations have the technical equipment necessary to detect a very weak signal. Detection is aided by good operating conditions (low latitude, high altitude, good atmospheric seeing and the absence of humid haze). Additional stations should contribute to lunar ranging campaigns (see Fig. 2 for measurement statistics).

The up-leg divergence is limited by atmospheric turbulence (seeing), so that one may not expect better than about 1 as (5 μ rad) divergence illuminating a 2-km spot on the Moon, translating to about 3×10^{-8} throughput onto the smaller Apollo 11 and 14 arrays. The down-leg divergence is set by diffraction from the corner cubes. The Apollo cubes produce a central irradiance that is roughly one-fifth that of a top-hat illumination with diameter λ/D corresponding to the circular aperture of diameter D and laser wavelength λ , so that each square meter of aperture on Earth receives about 7×10^{-9} of the flux incident on the reflector. The net throughput is then $\approx 2 \times 10^{-16}$ for each square meter of aperture on Earth. Adding to this typical optical system and atmospheric throughputs (traversed twice), together with filters and detection efficiencies, total throughput tends to be in the range of 10^{-18} per square meter of aperture on Earth. An energetic pulse of laser light having a pulse width in the neighborhood of 100 ps might have an energy of 100 mJ, corresponding to 3×10^{17} photons at green wavelengths. The result is that LLR invariably operates in the single-photon detection regime. Further degradation owes to poor atmospheric seeing (the calculation here is for 1 arcsecond, which is rarely achieved for many of the LLR ground stations) in addition to an estimated factor-of-ten degradation of the reflector arrays over time as reported by Murphy et al. (2010).

In practice, the Apache Point station's best performance collects about five photons per shot from the Apollo 15 reflector (Murphy 2013), while OCA's best performance is about 0.1 photons per shot and 0.02 photons per shot from MLRS—and similar to the Matera station. The original 2.7-m McDonald LLR station approached a single photon per pulse, but the photon rate was much lower due to a pulse repetition rate of 0.3 Hz (compared to 10 Hz for OCA and MLRS and 20 Hz for APOLLO). Prior to 2006, ranges to the larger Apollo 15 reflector dominated LLR data (roughly 85% of range measurements). APOLLO reduces dependence on Apollo 15 to less than half of measurements, and the recent addition of infrared capability at OCA evens out the distribution even more.

In low-signal regimes, it can be helpful to operate with a train of about five laser pulses per shot, as is practiced by the Wettzell station. A correlation of the laser pulse signature, derived directly from the laser cavity, with the histogram of all accumulated detector events within the range gate allows the Wettzell station to extract the coherently spaced lunar returns from the randomly distributed noise recordings.

Pointing and tracking a telescope to arcsecond precision on a target that provides virtually no feedback is a difficult challenge. The problem is exacerbated in conditions of excellent seeing and correspondingly small beam divergence. Although the signal may be much higher, a deliberate point ahead of the laser beam relative to the receiver direction of the order of one arcsecond is required due to relative tangen-

Fig. 1 Distribution of LLR normal points taken by the major observatories over the years

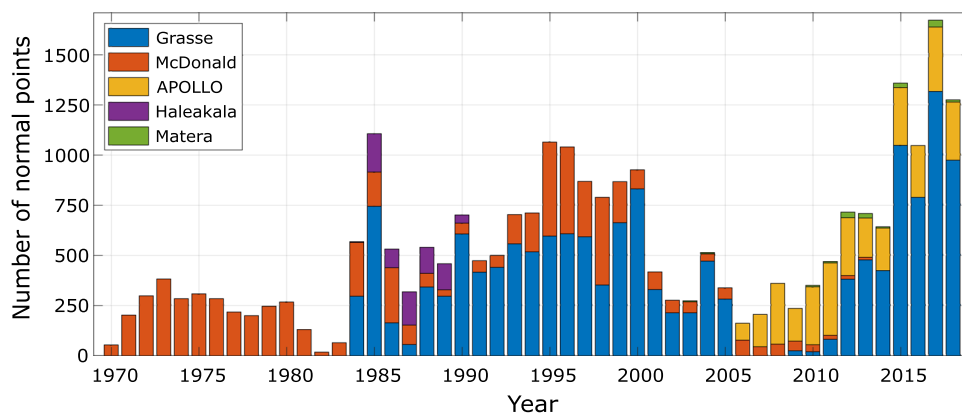
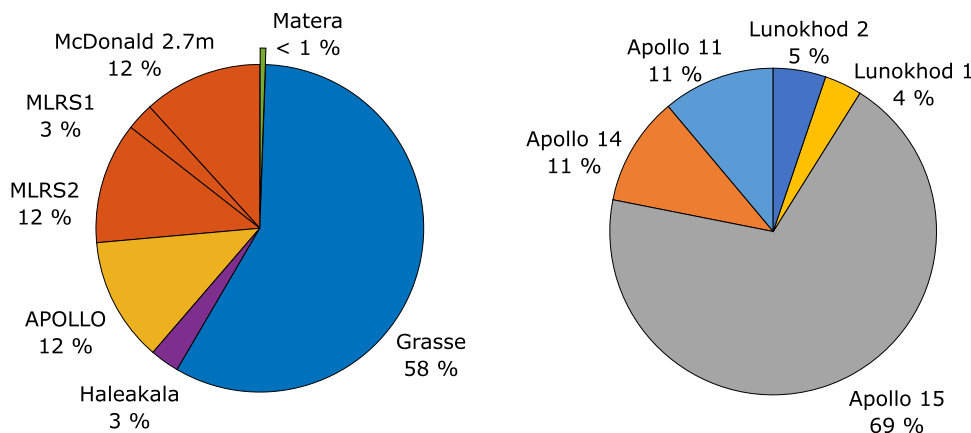


Fig. 2 Measurement statistics (1970–2018) with observatories (left), reflectors (right)



tial motion between the reflector and telescope. Additionally, the illuminated face of the Moon presents a high background that is most effectively filtered in the temporal domain by predicting the photon return time to a stability of approximately one nanosecond. Spatial and spectral filters also eliminate unwanted background light.

3.2 Example apparatus

Figure 3 illustrates the typical measurement equipment at an LLR site, here Wettzell. A full description of the latest implementation of an LLR apparatus can be found in Murphy et al. (2008b). In brief, APOLLO employs a 2.3 W average power laser at 532 nm, generating 100 ps pulses at a 20 Hz repetition rate and 115 mJ per pulse. The laser is transmitted from the 3.5 m aperture telescope at the Apache Point Observatory in southern New Mexico at an elevation of 2.8 km. The full aperture is utilized for beam transmission. A small portion of the outgoing beam is intercepted by a corner cube prism attached to the telescope secondary mirror, sending light back to the receiver, attenuated to the single-photon level and providing a precise measure of the pulse departure time.

The receiver (detector) houses a 4 × 4 avalanche photodiode (APD) array capable of high-precision timing of single photons at a detection sensitivity around 30%. Photon arrivals

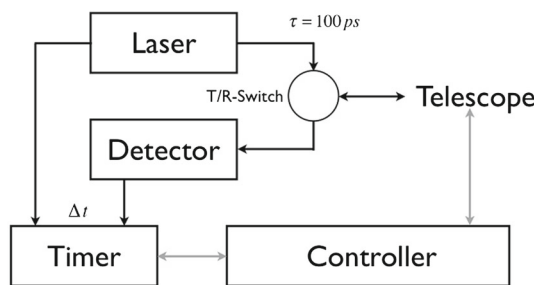


Fig. 3 Principal measurement equipment at the LLR observatory Wettzell

create START pulses for a 16-channel time-to-digital converter (TDC) with 15 ps jitter and 25 ps bins. STOP pulses to the TDC are extracted from a 50 MHz low-phase-noise clock pulse train, and the number of clock pulses between the STOP signal for the local corner cube return and the STOP signal for the lunar return is counted. The master clock on which the 50 MHz pulse train is generated uses an ovenized quartz crystal disciplined by the global positioning system (GPS) so that the 2.5-s round-trip travel time is measured against a reliable frequency standard. The absolute time delivered by this system is known far better than the microsecond level required for millimeter range precision.

A recent development adds an absolute calibration capability to APOLLO, permitting millimeter accuracy and not just precision. The system is based on a fiber laser delivering 10 ps pulses at 80 MHz and locked to a cesium clock so that pulse intervals are known/trusted at the few-picosecond level over several seconds of time. Injecting the 532-nm photons from selected pulses onto the APD detector array during LLR acquisition permits real-time optical “tick marks” against which to measure lunar return photons. A single five-minute LLR run on one reflector is thus able to collect enough calibration data to determine measurement accuracy below the one-millimeter level (Adelberger et al. 2017).

3.3 Lunar Laser Ranging in infrared

For many years, LLR observations using a green wavelength have suffered an inhomogeneity problem both temporally and spatially. A new infrared (IR) detection capability at the Grasse LLR station improves this situation (Courde et al. 2017). The implementation of IR detection for LLR provides new opportunities for the improvement in scientific products. As expected, LLR in infrared increases the station efficiency by a factor of eight during new and full Moon periods and improves the temporal homogeneity of LLR observations over a synodic month, as shown in Fig. 4. The best link budget at this wavelength results in a significant increase in the normal points (NPs, see Sect. 3.4) over all the reflectors on the Moon. The observations are statistically more homogenous over all the targets, as shown in Fig. 4. A surprising result concerns the Lunokhod 2 array behavior in IR. The degradation of Lunokhod 2 performances compared to Lunokhod 1 seems to be chromatic because the significant difference observed in green at Grasse and APOLLO is absent in IR (Murphy et al. 2011; Courde et al. 2017). Although this difference remains unexplained, the differential reflectivity at those two separate wavelengths gives new insights to analyze the performances of lunar retroreflectors.

3.4 Observations and data reduction

LLR observations are conducted to one reflector at a time, each observation typically dwelling for 5–15 min. In this time, anywhere from a few lunar photons to thousands may be recorded. Because the dynamics of the Earth–Moon system within this short span is not of interest to LLR science, the series of individual-shot observations is consolidated into a single representative launch time and associated round-trip travel time. This measurement pair—together with representative meteorological information and other auxiliary data—is packaged into a data unit called a normal point.

Identifying the legitimate lunar returns in the presence of a high noise background is accomplished by first subtracting a high-fidelity prediction/model from the measured round-

trip time so that the legitimate returns lie in an identifiable line, although likely having an offset and small slope due to model imperfections (Abbot et al. 1973), also see Fig. 5. To the extent that any residual slope is small, a histogram of the entire data set will often reveal the signal. Photoelectron events within a prescribed narrow window of the histogram peak may be considered valid, though additional noise filtering techniques may also be employed. Once identified, the returns may be fit with a linear or (with caution) higher-order polynomial, acting to simultaneously average the returns and establish the model offset at arbitrary time. It is then possible to select a representative launch time—which need not correspond to an actual launch time—and assess the value of the model plus fit offset at that time. The result becomes the round-trip time reported in the normal point.

4 Modeling and analysis

As an example of LLR analysis and parameter estimation, the analysis model used at Institut für Erdmessung (IfE) is briefly described. Similar procedures are implemented at other International Laser Ranging Service (ILRS) LLR analysis centers (e.g., Williams et al. 2009, ILRS annual reports¹). The basis for the analysis of LLR data in Germany was developed in the late 1980s and 1990s at Technical University of Munich (Müller 1991) and recently further improved (Biskupek 2015; Hofmann 2017; Hofmann and Müller 2018).

The IfE model is fully relativistic up to the first post-Newtonian order. It has an accuracy level of about 1–2 cm for reconstructing the real distance between observatories on the Earth and five retroreflector arrays on the Moon, see Müller et al. (2014) for an overview. The LLR analysis software package consists of two major modules: i) computation of the ephemerides of the main solar system bodies; ii) global parameter adjustment where improved values of the unknowns and the corresponding formal standard errors are obtained. The dynamical partials, i.e., those that depend on the position of Earth, Moon and Sun, are calculated by finite differences of numerically integrated ephemerides.

The modeling of the light travel time τ is done separately for the up leg τ_{12} and down leg τ_{23} with $\tau = \tau_{12} + \tau_{23}$ at the times t_1 , t_2 and t_3 for emission, reflection and reception of the laser pulse:

$$\begin{aligned}\tau_{12} &= \frac{1}{c} |\mathbf{r}_M(t_2) + \mathbf{r}_{\text{ref}}(t_2) - \mathbf{r}_E(t_1) - \mathbf{r}_{\text{obs}}(t_1)| + \Delta\tau_{12} \\ \tau_{23} &= \frac{1}{c} |\mathbf{r}_E(t_3) + \mathbf{r}_{\text{obs}}(t_3) - \mathbf{r}_M(t_2) - \mathbf{r}_{\text{ref}}(t_2)| + \Delta\tau_{23} \quad (1)\end{aligned}$$

¹ <https://ilrs.cddis.eosdis.nasa.gov/about/reports>.

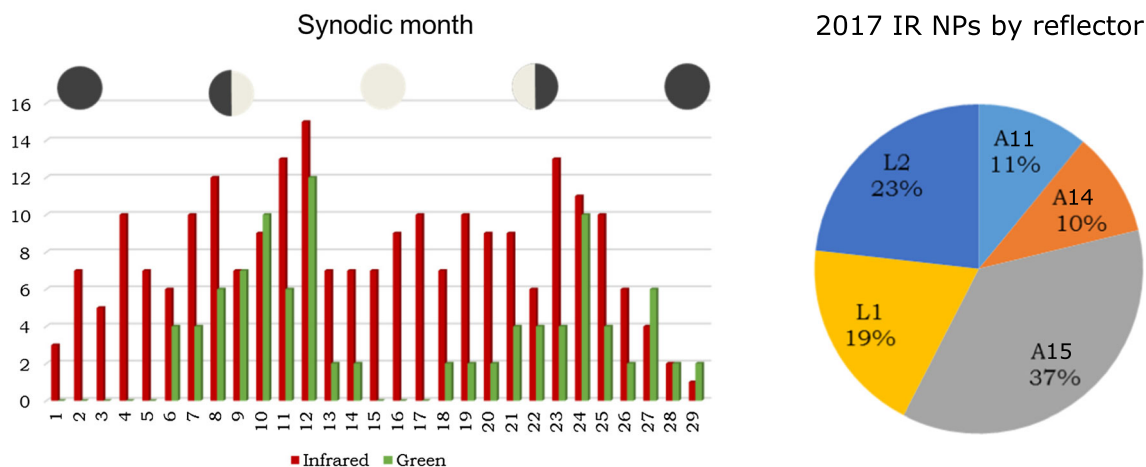


Fig. 4 Repartition of the normal points during the synodic month—normal points statistics by reflector (Apollo and Lunokhod)

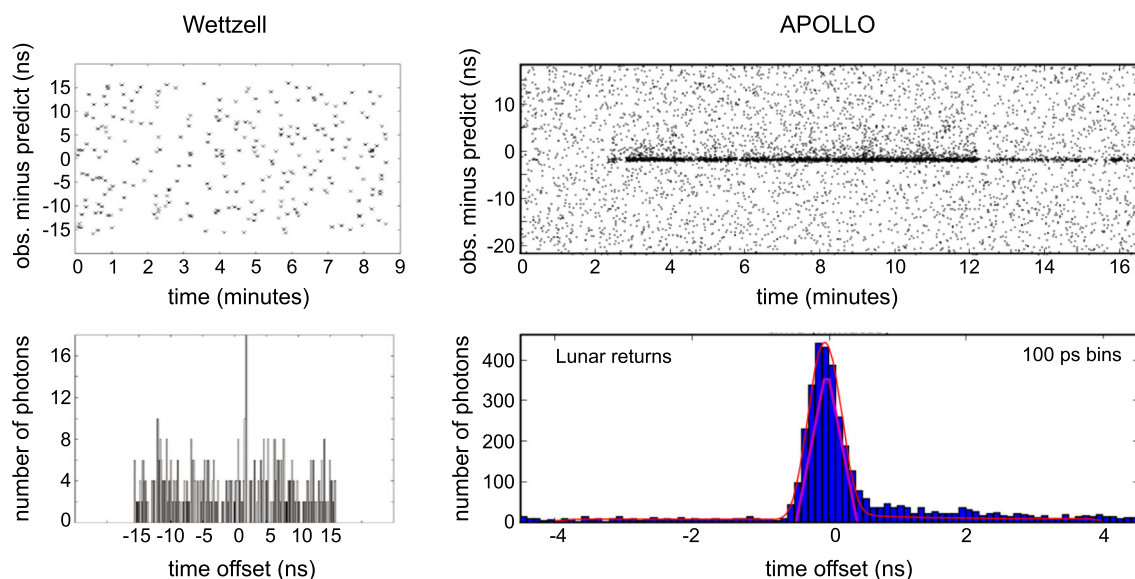


Fig. 5 Lunar returns (observed minus computed residuals) as a time series showing a lot of background noise (upper panels) and in histogram representation (lower panels). On the left-hand side a typical lunar measurement at Wetzell is shown and on the right-hand side a typical scenario for the APOLLO site

with the speed of light c , vector of geocenter \mathbf{r}_E and selenocenter \mathbf{r}_M in the solar system barycentric (SSB) frame, the position vector of the observatories from the center of the Earth \mathbf{r}_{obs} , the position vector of the reflectors from the center of the Moon \mathbf{r}_{ref} and leg-dependent delays $\Delta\tau_{12}$, $\Delta\tau_{23}$ due to atmospheric and relativistic effects as well as station dependent biases. To apply Eq. (1), all vectors and measured times must be given in the same inertial reference frame. The vectors \mathbf{r}_{obs} and \mathbf{r}_{ref} are transformed from their original terrestrial (TRF) or selenocentric (SRF) reference frames into the SSB frame (Soffel et al. 2003). The real LLR measurement fundamentally consists of recording two event

times—corresponding to photon launch and detection—on a terrestrial clock synchronized to the atomic clock ensemble that defines atomic time (TAI), for instance. Measured times are transformed into the SSB frame following the IERS Conventions 2010 using the time ephemeris TE405 (Petit and Luzum 2010; Harada and Fukushima 2003). Another recent time ephemeris can be found in Viswanathan et al. (2017).

The rotation matrix between the TRF and inertial frame is calculated from the Earth orientation parameters as described in Petit and Luzum (2010). For the rotation between SRF and inertial frame, the lunar orientation is required, which is obtained by numerical integration of the Euler–Liouville

equations for the Moon, where also external torques caused by other solar system bodies as well as relativistic torques due to geodetic and Lense–Thirring precession are taken into account (Thorne and Hartle 1985). The IfE model for lunar libration comprises a model with an elastic, homogeneous and dissipative Moon including the influence of a liquid core according to JPL DE430 ephemeris (Williams and Boggs 2009; Folkner et al. 2014; Hofmann and Müller 2018).

The Earth and Moon vectors \mathbf{r}_E and \mathbf{r}_M in Eq. (1) are calculated by numerical integration of the relativistic Einstein–Infeld–Hoffmann equations of motion in harmonic coordinates to seek world lines of the relevant bodies that satisfy the round-trip light propagation measurements in the SSB frame. Introducing some parametrized post-Newtonian (PPN) framework, one might look for violations of general relativity (GR) by means of LLR data, as described in Williams et al. (1996a) and Müller et al. (2008b). Added to the point–mass attractions between solar system bodies are Newtonian accelerations due to gravity field inhomogeneities of Earth and Moon, as well as the secular tidal acceleration of the lunar orbit. The JPL integration model for orbit and lunar rotation is described in Standish and Williams (2012) and Folkner et al. (2014). The Institute of Applied Astronomy model is described by Pavlov et al. (2016), and the model for the INPOP ephemeris is described in Manche (2011) and Viswanathan et al. (2018).

For the estimation of model parameters in the Earth–Moon system, the model is adjusted to the observations by performing a weighted least-squares fit. A typical standard solution covers the (non-relativistic) Newtonian parameters, which are estimated in a first run of the analysis, by fixing other tiny parameters (like relativistic quantities, etc.) to their state-of-the-art (e.g., Einsteinian) values until a stable solution is obtained. These solution parameters include coordinates and velocities of LLR observatories and retroreflectors, initial values for the lunar orbit and rotation, $GM_{\text{Earth+Moon}}$, long-periodic nutation coefficients, initial values for the lunar orbit and rotation, some mass multipole moments of the Moon (C_{22} in combination with dynamical β , C_{32} , C_{33} , S_{32} , but different choices can be made), lunar Love numbers k_2 and h_2 , parameters related to dissipation effects in the lunar interior as well as time delays of solid Earth tides indicating the lunar tidal acceleration and measurement biases (Hofmann 2017; Hofmann et al. 2018). After convergence is achieved, certain parameters like single relativistic parameters (e.g., equivalence principle parameter, possible temporal variation of the gravitational constant, cf. Hofmann and Müller 2018) are estimated together with the Newtonian parameters. All other relativistic parameters are fixed to their Einsteinian values. Examples for recent estimates of various parameters in the Earth–Moon system are discussed in the following section.

5 Results

5.1 Tests of gravity

The lunar orbit provides a pristine laboratory for testing gravity, as non-gravitational effects on the orbit begin to show up only at the millimeter level (e.g., Vokrouhlicky 1997). Moreover, the Moon is far enough from the Earth to be strongly perturbed by solar gravity. This fact permits the Earth–Moon–Sun system to be used as a probe of the equivalence principle (and other relativistic phenomena) at scales of 1 AU—extending the baseline against which to compare the raw measurement precision.

We highlight here some of the contributions to gravitational physics from LLR. Most of these science results are based on modeling that currently produces post-fit residuals of measured data in the neighborhood of 1–2 cm, so that millimeter-quality data could in principle improve current limits by an order of magnitude given commensurate improvements in modeling and analysis.

5.1.1 Equivalence principle

The simplest prediction of Einstein’s equivalence principle (EP)—the universality of free-fall—is one of the most precisely tested principles in all of physics. Yet there are strong motivations for extending the tests and pushing their precisions even higher. The EP comes in two key forms. The weak form of the EP (WEP) applies to the gravitational properties of everything but gravity itself, while the strong EP (SEP) accounts for gravity. Besides binary pulsars (e.g., Damour and Schäfer 1991), the Earth–Moon system is among the best available probes of the SEP as was first pointed out by Nordtvedt (1968a, b, c). From the vantage point of the EP, the Earth and Moon are test bodies that differ in two important ways. First, the Earth’s mass has a fractional contribution from gravitational self-energy (4.6×10^{-10}) that is about 20 times greater than that of the Moon—allowing LLR to test the SEP. Second, the Earth has a massive iron–nickel core, while the Moon is dominated by silicates similar to the Earth’s mantle—making LLR sensitive to a WEP violation as well. Laboratory WEP tests of Earth-like and Moon-like objects falling toward the Sun can be used to distinguish between Earth–Moon SEP and WEP violations (Baeßler et al. 1999).

LLR tests the SEP by measuring the difference in the accelerations of the Earth and Moon toward the Sun. In the presence of a differential acceleration, the orbit of the Moon—from our perspective on the Earth—would appear to be displaced, or polarized, toward or away from the Sun. The range signal would take the form

$$\Delta r = 13.1\eta \cos D \text{ [in meters]} \quad (2)$$

where D is the lunar orbit's synodic phase having a period of 29.53 days, with $D = 0$ corresponding to new Moon (Nordtvedt 1995; Damour and Vokrouhlický 1996). The parameter η is a theory-dependent dimensionless coefficient sensitive to almost every post-Newtonian feature of the theory. Although η vanishes in GR, it generally does not in alternative theories. But independent of any theory, this test of the SEP addresses a very basic and important question—What is the weight of gravity itself? It tests a crucial nonlinear property of gravity: How gravity produces energy that itself gravitates.

The metric models by Damour and Nordtvedt (1993) describe a relaxation of scalar field strength that today would produce SEP differential accelerations between 5×10^{-17} and 10^{-13} . The present limit on differential acceleration is in the order of $\Delta a/a = \pm(0.5 \dots 1.3) \times 10^{-13}$ (Williams et al. 2012; Viswanathan et al. 2018; Hofmann and Müller 2018), corresponding to a test of the SEP at the level of $|\eta| < 3 \times 10^{-4}$, given the self-energy fraction of the Earth. Millimeter-quality ranging stands to improve sensitivity of the SEP test by one order of magnitude, measuring $\Delta a/a$ to a precision of 10^{-14} and reaching into the theoretically motivated range indicated above.

5.1.2 Time variation of the gravitational constant

A secular change in the gravitational constant, G , would produce secular changes in the lunar mean distance and the orbital period (Kepler's third law), as well as in the angular rate of the Earth about the Sun. While the orbital semimajor axis change results in a range signal that varies linearly in time, the change in orbital period leads to a quadratic evolution of the Moon's mean anomaly (phase) with time. Similar behavior caused by tidal dissipation prevents that evolution from being unique, but the solar perturbations give a more identifiable signal. The solar orbit longitude also has a quadratic time dependence that powerfully constrains \dot{G}/G through the solar perturbations of the lunar orbit (Williams et al. 1996b). Here, the long time span of LLR measurements becomes important, limiting \dot{G}/G at the impressive level of less than three parts in 10^{13} per year (Williams and Folkner 2009; Hofmann and Müller 2018).

Steinhardt and Wesley (2010) examined the constraints that observations and experiment place on a wide range of ideas for explaining dark energy in the context of extra-dimensional theories. They find that if current constraints on both \dot{G}/G and the value and rate-of-change of the equation-of-state parameter, w , improve by a factor of two, such ideas could be ruled out at the 3σ level. In their analysis, Steinhardt and Wesley use the pulsar timing \dot{G}/G limit of 6×10^{-12} 1/years. LLR already improves on this limit by more than a factor of ten.

5.1.3 Gravitomagnetism, geodetic precession and other PPN tests

LLR tests a number of basic relativistic phenomenologies. These phenomena include gravitomagnetism, geodetic precession and consequences of preferred frames. Many such phenomena can be cast into the parameterized post-Newtonian (PPN) framework (Nordtvedt and Will 1972; Will 1993): a generalized metric description of gravity for which GR is a special case. The most prominent PPN parameters are γ , describing the amount of curvature produced per unit mass, and β , describing the nonlinearity of gravity. Both of these are unity in GR. The best constraint on γ comes from Doppler tracking of the Cassini spacecraft: $|\gamma - 1| < 2.3 \times 10^{-5}$ (Bertotti et al. 2003). β is constrained by LLR tests of the SEP via the identity: $\eta = 4\beta - \gamma - 3$. Using the Cassini result for γ with the LLR result for η yields $|\beta - 1| < 6 \times 10^{-5}$ (Hofmann and Müller 2018). Recently, interplanetary ranging to mercury has improved on the LLR β result (Park et al. 2017; Genova et al. 2018).

Gravitomagnetism is a generic consequence of any mass in motion. As the Earth orbits the Sun, its gravitomagnetic field exerts a Lorentz force on the Moon. If the gravitomagnetic force in the BCRS were missing while the other GR terms were present, it would cause 6-m-amplitude periodic disturbances (in harmonic coordinates) at both synodic and twice-synodic frequencies that are not seen (Murphy et al. 2007; Murphy 2009). The LLR analysis constrains this effect to less than 0.2 % precision, as confirmed by Soffel et al. (2008). Note: The gravitomagnetic effect as studied in our case is coordinate dependent (Kopeikin and Xie 2010). Thus, it is not the gravitomagnetic field which is measured but the self-consistency of the set of relativistic equations. The coordinate-independent gravitomagnetic effect is small (less than 1 mm) but might be observed with better LLR data in future (Kopeikin 2010). A direct measurement of the frame dragging as component of gravitomagnetism was done by the LAGEOS-LARES and Gravity Probe B experiments (Ciufolini et al. 2016; Everitt et al. 2011).

Geodetic precession, at 19.2 mas/years, is tested by LLR (Williams et al. 1996b; Turyshev and Williams 2007; Hofmann and Müller 2018) and is now confirmed at the 0.1...0.3 % level. LLR measures the radial distance between Earth and Moon and can determine the rotation rates of the lunar perigee with respect to space which is strengthened by an accurate planetary ephemeris (Williams et al. 1996b). The spatial orientation of the used fundamental reference systems (barycentric, geocentric and selenocentric reference systems) is tied to the International Celestial Reference System (ICRS) realized by Very Long Baseline Interferometry (VLBI) observations. Geodetic precession is likewise a measure of PPN γ .

Preferred-frame effects, such as those codified by PPN parameters α_1 and α_2 , are also tested by LLR, currently at the level of 2×10^{-5} and 9×10^{-6} , respectively (Hofmann 2017; Müller et al. 1996) with the cosmic microwave background as preferred frame, although Nordtvedt (1987) obtains a stronger limit on α_2 based on the long-term orientation of the spin axis of the Sun.

5.1.4 Lorentz symmetry in the standard-model extension parametrization

Lorentz symmetry is a fundamental symmetry of space–time. It assumes that the result of any local test experiment is independent of the velocity and the orientation (in space and time) of the inertial frame in which the experiment is conducted (Will 2014). The Lorentz symmetry is satisfied in any sectors of Physics; in quantum Physics, it is seen as a global property of overall space–time while it becomes a local property in general relativity through the EP. In an effort to turn general relativity into a quantum field theory, some unification theories predict a breaking of Lorentz symmetry at different energy levels. In an attempt to test this possibility, Colladay and Kostelecký (1997, 1998) have built an effective field theory framework which parametrized any Lorentz symmetry violations in all sectors of Physics. This wide framework is called the standard-model extension (SME) and possesses hundreds of coefficients (all are equal to zero in General Relativity) to be determined by direct confrontation with experiments.

The main motivation for studying Lorentz symmetry violations in the SME framework compared to the PPN framework is related to the fact that (i) it does not possess overlapping coefficients with the PPN framework as pointed out by Bailey and Kostelecký (2006) and (ii) it offers the possibility to test non-metric theories of gravity. Indeed, in the matter sector of the SME, violations show up through couplings between matter and the Lorentz violating fields. Also, in the point-mass limit, test bodies do not follow geodesics of space–time anymore. Their motions become species dependent and lead to violations of the WEP.

The first test in the pure gravitational sector of the minimal SME using LLR data was performed by Battat et al. (2007). They provided six null estimations (from 10^{-6} to 10^{-11}) on six linear combinations of SME coefficients. They used analytical signatures derived by Bailey and Kostelecký (2006) that they fitted directly in LLR residuals previously obtained in the pure general relativity framework. More rigorously, Bourgoïn et al. (2016) have included directly Lorentz symmetry violations into a LLR data analysis software similar to the one described in Sect. 4. They have shown that the linear combinations of SME coefficients to which the LLR data are sensitive to are different from the analytical ones used in Battat et al. (2007). They provided six realistic con-

straints at the level 10^{-8} up to 10^{-12} . This test is among the best constraints to date in the pure gravitational sector of the minimal SME. More recently, Bourgoïn et al. (2017) added Lorentz symmetry violations from matter–gravity couplings in order to test the WEP. Assuming very simple modeling for the composition of the Earth and the Moon, they provided the highest constraints to date simultaneously on the SME coefficients from the pure gravitational sector and the point-mass limit in the matter sector.

5.1.5 Inverse square law, extra dimensions and other frontiers

Any deviation from the Newtonian $1/r^2$ force law produces a precession of orbit perigees. LLR's measurement of any anomalous precession rate of the lunar orbit (within VLBI realized ICRS) limits the strength of Yukawa-like long-range forces with ranges comparable to the $\approx 10^8$ m scale of the lunar orbit to $< 5 \times 10^{-11}$ times the strength of gravity. This is the strongest available constraint on the inverse square law (Adelberger et al. 2003; Hofmann 2017).

Measurement of the precession rate can also probe a recent idea (called DGP gravity) in which the accelerated expansion of the universe does not arise from a nonzero cosmological constant but rather from a long-range modification of the gravitational coupling, brought about by higher-dimensional effects (Dvali et al. 2003a, b; Lue and Starkman 2003). Even though the lunar orbit is far smaller than the Gigaparsec length-scale characteristic of the anomalous coupling, there would be a measurable signature of this new physics, manifesting itself as an anomalous precession rate at about 5 $\mu\text{s}/\text{years}$ —roughly a factor of ten below current LLR limits, and potentially reachable by millimeter-quality LLR.

5.2 Geophysics

Concerning “terrestrial” parameters, LLR mainly contributes to monitoring long-term variations of Earth orientation parameters EOP (i.e., precession and nutation as well as Earth rotation and polar motion). For example, precession rate and nutation coefficients of different periods (18.6 and 9.3 years, 1 year, 182.6 and 13.6 days) have been determined and analyzed with respect to the values of the MHB2000 model of Mathews et al. (2002). Hofmann et al. (2018) obtained discrepancies to the nutation model of up to 1.46 mas. The discrepancies shall be further studied by joint analysis with VLBI data. LLR determinations of the precession rate of the Earth's equator are compatible with the IAU model (Hilton et al. 2006). Zerhouni and Capitaine (2009) showed that it is possible to determine celestial pole offsets from LLR, however with less accuracy than results from VLBI because of fewer LLR observatories and data.

In the past, most often the daily decomposition method (Dickey et al. 1985) was applied to determine corrections for Earth rotation ΔUT0 and variation of latitude $\Delta\varphi$, where the post-fit residuals of the standard LLR solution were processed. In the last years, there were attempts to estimate a single Earth rotation parameter (x_p , y_p , or ΔUT) together with standard solution parameters for single nights, providing possible correlations with other parameters in the Earth–Moon system (Müller et al. 2015; Hofmann et al. 2018). Biskupek et al. (2009) estimated the pole coordinates x_p , y_p for longer time spans, indicating long-periodic variations in Earth orientation. They determined a drift rate in the pole coordinates to be 4.9 ± 0.3 mas/years for the full period of LLR data with fixed station velocities based on ITRF values, whereas Gross and Vondrák (1999) obtained a linear drift of 4.123 ± 0.002 mas/years, analyzing a shorter time series and also including non-LLR data. A denser network of LLR stations and simultaneous observations from different stations would be helpful to estimate EOP from LLR in future. LLR-based EOP results (ΔUT0 , $\Delta\varphi$) contribute to combined EOP solutions like JPL KEOF (Ratcliff and Gross 2018). The long time span of LLR data also provides the prerequisite to monitor long-term variations of the involved reference systems (see below).

Finally, the lunar tidal acceleration should be mentioned. It causes a secular increase in the average Earth–Moon distance by 3.82 cm/years and a $-25.9''/\text{cy}^2$ acceleration in orbital longitude (Chapront et al. 2002; Williams and Boggs 2016), which can only be determined accurately using LLR.

5.3 Selenophysics

The physical properties of the Moon affect its solid-body tides, physical librations and orbit. Since LLR is sensitive to all of these, there is opportunity to determine several parameters related to lunar physical properties. LLR stations range to five retroreflectors at different locations on the Moon, see Fig. 6. A broad geographical distribution of lunar sites aids the separation of range variations due to tidal displacements and physical librations from those due to orbit variations.

Solid-body tides at the lunar surface cause vertical displacements of about 0.1 m and horizontal displacements about half that. The two largest periodic tides have monthly periods and are of similar amplitude. The beat period between the two terms is 6 years, and the pattern of tides takes 6 years to nearly repeat. The Love number h_2 scales the vertical displacement and l_2 scales the horizontal. Fixing l_2 at a model value of 0.0107, the distribution of sites is not wide enough for good separation of l_2 from h_2 . A recent LLR analysis with data from 1970 to 2013 gives $h_2 = 0.043$ (Pavlov et al. 2016).

Torques on the Moon cause small variations in orientation called physical librations while also making the rotation

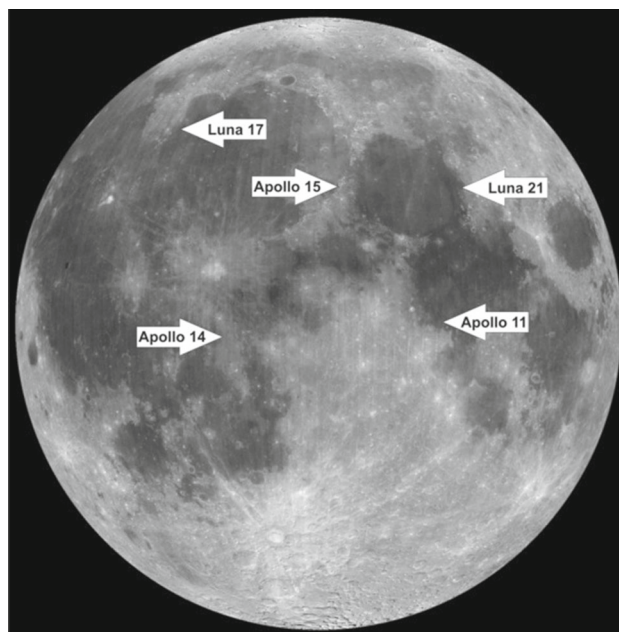


Fig. 6 Retroreflector arrays on the lunar surface. The Lunokhod 1 and 2 retroreflectors were landed by the Luna 17 and 21 missions, respectively

synchronous and causing an 18.6-year precession of the equator plane along the ecliptic plane. By being sensitive to these variations, LLR has determined moment of inertia differences, third-degree gravity field, Love number k_2 , tidal dissipation and interactions at the fluid-core/solid-mantle boundary. For the principal moments of inertia ordered $A < B < C$, LLR determines the difference combinations $(B - A)/C = 2.277 \times 10^{-4}$ and $(C - A)/B = 6.310 \times 10^{-4}$. Uncertainty in the last digit, with a relative uncertainty of 3×10^{-4} for both combinations, comes mainly from the poorly known moment of inertia of the fluid core. Compared to the Earth, the slowly rotating Moon is less oblate while the equatorial moments are less similar, so the Moon is triaxial. The moment difference combinations are related to the degree-2 gravity field. LLR is also sensitive to the degree-3 gravity field.

Although the potential Love number k_2 affects the physical librations and can be determined from the LLR data, the GRAIL mission has provided an accurate value of $k_2 = 0.0242 \pm 0.0002$ (Williams et al. 2014). Tides in the Moon are subject to dissipation that cause phase shifts in the tidal response. Along with k_2 , LLR determines a time delay for the tidal response and several tidal dissipation related terms. Following the procedure in Williams and Boggs (2015), the specific dissipation yields $Q = 38 \pm 4$ for monthly tidal periods and $Q = 41 \pm 9$ at one year. The time delay dissipation model has $k_2/Q \propto 1/(\text{Tidal Period})$. The solution for several perturbed periodic libration components allows more complex tidal models to be constructed. These post-fit models peak at 3–4 months, decreasing for longer and shorter

tidal periods. Also, dissipation should cause k_2 to increase with period.

In addition to tidal dissipation, the physical librations show dissipation arising from relative motion at the fluid-core/solid-mantle boundary (CMB). This evidence for a fluid lunar core was originally published in Williams et al. (2001). The dissipation can be explained as arising from a turbulent boundary layer by using the theory of Yoder (1995). The detection of CMB dissipation is now very strong (Williams and Boggs 2015), and LLR gives clear evidence of a fluid lunar core.

The orbit of the Moon and the physical librations are integrated numerically to achieve the high accuracy needed. The LLR analyses include the initial conditions for the orbit and physical librations. Given its age and the absence of oceans and atmosphere, one might expect the Moon's rotation to be completely damped by the dissipative effects leading to predictable initial conditions. But despite two strongly observed sources of dissipation, the physical librations exhibit two strongly detected free libration modes (Newhall and Williams 1997; Rambaux and Williams 2011; Yang et al. 2017). One mode is a 74.6-year wobble of the pole analogous to the Earth's Chandler wobble and the other is a 2.9-year longitude libration, a periodic variation in the rotation rate. The free libration modes affect the numerically integrated librations through the initial conditions. The modes may have been stimulated by resonance passage for the 2.9-year longitude libration (Eckhardt 1993) and turbulent core–mantle interactions for the wobble mode (Yoder 1981). Both deserve further investigation. In addition, weaker modes including core modes (Barkin et al. 2014; Petrova et al. 2018) are possible.

This section gives a brief description of lunar science obtained from LLR analysis. More extensive discussions are given in Williams and Boggs (2009), Williams and Boggs (2015) and Williams et al. (2014).

5.4 LLR contribution to celestial reference frames

The mean equator is not exactly aligned with zero declination in the International Celestial Reference Frame (ICRF), and zero right ascension is not quite at the intersection of the equator and ecliptic planes. Modern lunar numerical ephemerides are constructed by fitting dynamical models to the LLR observations: IfE model (Müller et al. 2014; Hofmann et al. 2018; Hofmann and Müller 2018), JPL DE (Folkner et al. 2014), EPM (Pitjeva and Pavlov 2017), ELPN (Bourgoin et al. 2016) and INPOP (Viswanathan et al. 2018). The LLR ephemerides realized by these numerical integrations are compatible with the ICRF, but we want to know the orientation of the equator and ecliptic in the ICRF. The LLR technique is particularly sensitive to the orientation of the mean equator plane and the mean ecliptic plane in the dynamical

reference frame defined from analytical or numerical solutions of planetary and lunar motions. Thus, LLR observations can be used to locate the mean ecliptic, mean equator and the mean equinox of J2000.0 in the extragalactic frame of the ICRF. This frame tie was achieved in three ways by Folkner et al. (1994): (1) by jointly reducing VLBI observations of planet-orbiting spacecraft and LLR observations; (2) by jointly reducing VLBI observations of quasars and LLR observations with a compatible transformation between the terrestrial frame (ITRF) and celestial frame (ICRF) and then comparing ground station positions; (3) by comparing pulsar timing positions that depend on the ephemeris of the Earth with VLBI positions.

Standish (1981) showed that two ways of defining the mean ecliptic plane have been used: one with a fixed reference frame and the other with a frame rotating with the mean ecliptic plane. The Paris Observatory Lunar Analysis Centre (POLAC) has examined this issue using an inertial mean ecliptic. In this study, the position of the inertial dynamical mean ecliptic of J2000.0 with respect to an equatorial frame chosen as reference is oriented by two angles: ϵ , the inclination of the ecliptic to the equator, and φ , the angle between the origin of the right ascension (o) on the equator and the ascending node (γ_{2000}^1) of the ecliptic on the equator (Fig. 7). Below, the link with ICRS is defined by the angles $\epsilon^{(\text{ICRS})}$ and $\varphi^{(\text{ICRS})}$, and in the same way, the angles $\epsilon^{(\text{Eq2000})}$ and $\varphi^{(\text{Eq2000})}$ define the link of the inertial dynamical mean ecliptic of J2000.0 with the mean equator of J2000.0 associated with the celestial pole (CEP or CIP). In these LLR analyses, the dynamical inertial mean ecliptic of J2000.0 is materialized with the lunar semi-analytical solution ELP2000-96 (Chapront et al. 1999) and the determination of the angles ϵ and φ depends on the precession–nutation matrix (PN) which is involved in the transformation between the terrestrial and the celestial system for the positions of the LLR tracking stations. If the reference is the ICRS, the PN matrix is constructed according to the IERS conventions using the celestial pole corrections ($\Delta\psi$, $\Delta\epsilon$ or ΔX , ΔY), given in the IERS EOP publications. If the reference is the mean equator of J2000.0, the PN matrix is built with modern analytical expressions: in the past, $P_{\text{Williams}}N_{\text{Herring}}$ (Williams 1994; Herring 1991) and more recently, $P_{\text{Capitaine}}N_{\text{Mathews}}$ (Capitaine et al. 2003; Mathews et al. 2002). The evaluations made by POLAC (Chapront et al. 2002) give the following values:

$$\begin{aligned}\epsilon^{(\text{ICRS})} &= 23^\circ 26' 21.4110'' \pm 0.1 \text{ mas}; \\ \varphi^{(\text{ICRS})} &= -55.4 \pm 0.1 \text{ mas}; \\ \epsilon^{(\text{Eq2000})} &= 23^\circ 26' 21.4056'' \pm 0.1 \text{ mas}; \\ \varphi^{(\text{Eq2000})} &= -14.6 \pm 0.1 \text{ mas}.\end{aligned}$$

The arc between $\gamma_{2000}^{1(\text{ICRS})}$ and $\gamma_{2000}^{1(\text{Eq2000})}$ on the ecliptic is $44.5 \pm 0.3 \text{ mas}$.

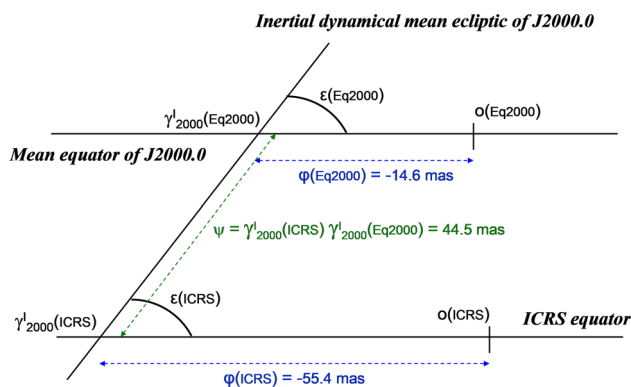


Fig. 7 Dynamical ecliptic plane orientation

The frame tie parameters improve with time, and LLR continues to improve the determination of the relative orientation of the ecliptic and equator planes. These results have some applications for the astronomical community. In the IAU 2009 System of Astronomical Constants (IAU 2009), the obliquity at J2000.0 is given under the notation ϵ_{J2000} and is equal to the value of $\epsilon^{(Eq2000)}$. It is also a component of the IAU 2006 precession model (Hilton et al. 2006). Note that while the VLBI technique alone allows a more accurate determination of the position of the mean equator of J2000.0 plane with respect to the ICRS equatorial plane (Herring et al. 2002), it does not allow determining the right ascension of the mean equinox of J2000.0 in the geocentric celestial reference system. This right ascension, noted $d\alpha_0$ in the IERS conventions (Petit and Luzum 2010), is equal to $\varphi^{(Eq2000)}$. Finally, LLR also contributes to terrestrial reference frame- and selenocentric reference frame-related parameters with station and reflector coordinates (Hofmann et al. 2018).

6 Future/outlook

Lunar Laser Ranging has stayed at the forefront of tests of gravity, probes of the lunar interior and determination of Earth coordinate systems. Recent improvements to the technique have stimulated a push to improve modeling capabilities, so we can expect further gains in the short term.

Longer-term improvements at the lunar end offer the biggest advantage—either in the form of new reflectors, active transponders or both. The current reflectors limit performance in a compounded way. Most fundamentally, the finite extent of the reflector array spreads the temporal width of the pulse by virtue of the fact that the array normal tilts away from the line of sight by up to 10° due to lunar libration. This spread can be as large as one nanosecond for the Apollo 15 array at full-tilt, corresponding to a root-mean-square measurement uncertainty of 50 mm for each returned photon. Statistical centroiding of the signal to millimeter-level

range precision requires hundreds or thousands of photons, which is how APOLLO achieves its goal. Courde et al. (2017) shows that also OCA with infrared measurements can get into the millimeter regime. Compounding this difficulty, while the weak signal associated with LLR has always been a limitation, reflector degradation over time has reduced the signal by a factor of approximately ten (Murphy et al. 2010). Thus, the brute force approach to LLR by gathering more photons is only getting harder.

Meanwhile, the spread imposed by the tilted reflector array eliminates incentive to improve ground-based laser pulse width or timing systems, since these errors add in quadrature to the dominant reflector spread. Improving APOLLO's 100-ps laser pulse width and 20-ps timing system—even by a factor of two—would have no discernible impact on the net timing precision and so would appear to be wasted effort. Scaling a new array also has no effect, as doubling both linear dimensions doubles the single-photon timing uncertainty, requiring four times the number of photons for \sqrt{N} statistical reduction to the same level—which is exactly what the quadrupled area of a double-sized array delivers: no precision gain.

Simply making a sparse array of corner cubes so that each one could easily be resolved by ≈ 100 ps laser pulses would break the logjam (Murphy 2013). Suddenly improvements in ground systems would have immediate impact. Halving the laser pulse width would require four times fewer photons for similar statistical precision. Most locations on the front face of the Moon see the Earth permanently well away from local zenith, so that a modest lateral separation on the ground (> 10 cm) is sufficient to separate the returns unambiguously.

Large single corner cubes have also been proposed (Otsubo et al. 2010; Currie et al. 2013; Turyshev et al. 2013). Such large cubes do not widen the reflected pulse, but they are more sensitive to thermal distortion and the diffraction pattern needs to be large enough to accommodate the velocity aberration of the laser beam.

Installing active laser transponders on the lunar surface would have perhaps an even greater impact on LLR science (Degnan 2008). Replacing the $1/r^4$ signal loss regime with a far more benign $1/r^2$ regime would allow the extensive SLR network to engage in LLR on a routine basis. This would have tremendous impact in data volume, global distribution (no LLR from the southern hemisphere, currently), tie-in to well-established geodetic stations, improvements in Earth surface/atmospheric models by having a reference unaffected by non-gravitational forces, etc. In this context, transponders work best in asynchronous mode, rather than echoing detected incoming signals. This permits the transponder to transmit a steady pulse train tied to a good clock and recording times of incoming signals with respect to this clock. The asynchronous mode has much greater noise immunity and thermal stability than echo-based techniques.

The accuracy of lunar science parameters depends on the spread of retroreflectors or transponders on the Moon. Figure 5 shows that a southern hemisphere target would be very useful and the northern hemisphere spread could be broadened. Signal strength, range accuracy and geometric distribution are all reasons to place new retroreflectors or transponders on the Moon.

Lunar Laser Ranging can be improved by refined modeling, very accurate ranging stations at a variety of terrestrial locations and widely distributed reflectors or transponders on the Moon. Future LLR will continue to contribute to science (Kopeikin et al. 2008).

Acknowledgements Some of the text contributed by T.W. Murphy is similar to the text in another review article by Murphy (2013); both that article and this one were originally solicited in the same month. Current LLR data are collected, archived and distributed under the auspices of the International Laser Ranging Service (ILRS) (Pearlman et al. 2002). We acknowledge with thanks that the more than 49 years of processed LLR data have been obtained under the efforts of the personnel at the Observatoire de la Côte d’Azur in France, the LURE Observatory in Maui, Hawaii, the McDonald Observatory in Texas as well as the Apache Point Observatory in New Mexico and the Matera Laser Ranging station in Italy. We would also like to thank the International Space Science Institute (ISSI, <http://www.issibern.ch/teams/lunarlaser>) in Bern for supporting this research. LLR-related research at the University of Hannover was funded by the DFG, the German Research Foundation, within the research units FOR584 “Earth rotation and global dynamic processes” and FOR1503 “Space-Time Reference Systems for Monitoring Global Change and for Precise Navigation in Space.” APOLLO results are based on access to and observations with the Apache Point Observatory 3.5-m telescope, which is owned and operated by the Astrophysical Research Consortium. APOLLO is jointly funded by the National Science Foundation (PHY-1404491) and the National Aeronautics and Space Administration (NNX-15AC51G). Portions of the research described in this paper were carried out at the Jet Propulsion Laboratory of the California Institute of Technology and the Center for Space Research of the University of Texas at Austin, under contracts with the National Aeronautics and Space Administration. US government sponsorship acknowledged.

References

- Abbot RI, Shelus PJ, Mulholland JD, Silverberg EC (1973) Laser observations of the Moon: identification and construction of normal points for 1969–1971. *Astron J* 78:784–793. <https://doi.org/10.1086/111484>
- Adelberger EG, Heckel BR, Nelson AE (2003) Tests of the gravitational inverse-square law. *Annu Rev Nucl Part Sci* 53:77–121. <https://doi.org/10.1146/annurev.nucl.53.041002.110503>
- Adelberger EG, Battat JBR, Birkmeier KJ, Colmenares NR, Davis R, Hoyle CD, Huang LR, McMillan RJ, Murphy TW, Schlerman E, Skrobol C, Stubbs CW, Zach A (2017) An absolute calibration system for millimeter-accuracy APOLLO measurements. *Class Quantum Grav* 34(24):245008. <https://doi.org/10.1088/1361-6382/aa953b>
- AFCLR (1969) Laser target on Moon works for air force scientists. *Bull Géodésique* (1946–1975) 94(1):443–444. <https://doi.org/10.1007/BF02522881>
- Baessler S, Heckel BR, Adelberger EG, Gundlach JH, Schmidt U, Swanson HE (1999) Improved test of the equivalence principle for gravitational self-energy. *Phys Rev Lett* 83:3585–3588. <https://doi.org/10.1103/PhysRevLett.83.3585>
- Bailey QG, Kostelecký VA (2006) Signals for Lorentz violation in post-Newtonian gravity. *Phys Rev D* 74(4):045001. <https://doi.org/10.1103/PhysRevD.74.045001>
- Barkin YV, Hanada H, Matsumoto K, Sasaki S, Barkin MY (2014) Effects of a physical librations of the Moon caused by a liquid core, and determination of the fourth mode of a free libration. *Sol Syst Res* 48(6):403–419. <https://doi.org/10.1134/S003809461406001X>
- Battat JBR, Chandler JF, Stubbs CW (2007) Testing for Lorentz violation: constraints on standard-model-extension parameters via lunar laser ranging. *Phys Rev Lett* 99(24):241103. <https://doi.org/10.1103/PhysRevLett.99.241103>
- Bender PL, Currie DG, Dicke RH, Eckhardt DH, Faller JE, Kaula WM, Mulholland JD, Plotkin HH, Poultney SK, Silverberg EC, Wilkinson DT, Williams JG, Alley CO (1973) The lunar laser ranging experiment. *Science* 182:229–238. <https://doi.org/10.1126/science.182.4109.229>
- Bertotti B, Iess L, Tortora P (2003) A test of general relativity using radio links with the Cassini spacecraft. *Nature* 425:374–376. <https://doi.org/10.1038/nature01997>
- Biskupek L (2015) Bestimmung der Erdrotation mit Lunar Laser Ranging. PhD thesis, Leibniz Universität Hannover, Deutsche Geodätische Kommission bei der Bayerischen Akademie der Wissenschaften, Series C 742. http://www.dgk.badw.de/fileadmin/user_upload/Files/DGK/docs/c-742.pdf
- Biskupek L, Müller J (2009a) Lunar Laser Ranging and Earth Orientation. In: Soffel M, Capitaine N (eds) *Proceedings of the “Journées 2008 Systèmes de référence spatio-temporels”*, pp 182–185, Dresden, Germany, 22–24 Nov 2008
- Biskupek L, Müller J (2009b) Relativity and Earth orientation parameters from lunar laser ranging. In: Schillak S (ed) *Proceedings of the 16th international workshop on laser ranging, 16th international workshop on laser ranging*, Poznan, Poland, 12–17 Oct 2008
- Biskupek L, Hofmann F, Müller J (2009) Pole coordinates from the analysis of LLR data. Poster at IERS workshop on EOP combination and prediction, Warsaw, 19–21 October 2009, Poland. <https://doi.org/10.15488/2654>
- Bizouard C, Lambert S, Becker O, Richard JY (2017) Combined solution C04 for Earth rotation parameters consistent with international terrestrial reference frame 2014. <http://hpiers.obspm.fr/eoppc/eop/eopc04/C04.guide.pdf>
- Bourgoin A, Hees A, Bouquillon S, Le Poncin-Lafitte C, Francou G, Angonin MC (2016) Testing Lorentz symmetry with lunar laser ranging. *Phys Rev Lett* 117(24):241301. <https://doi.org/10.1103/PhysRevLett.117.241301>
- Bourgoin A, Le Poncin-Lafitte C, Hees A, Bouquillon S, Francou G, Angonin MC (2017) Lorentz symmetry violations from matter-gravity couplings with lunar laser ranging. *ArXiv e-prints arXiv:1706.06294*
- Capitaine N, Wallace PT, Chapront J (2003) Expressions for IAU 2000 precession quantities. *Astron Astrophys* 412:567–586. <https://doi.org/10.1051/0004-6361:20031539>
- Chang RF, Alley CO, Currie DG, Faller JE (1972) Optical properties of the Apollo laser ranging retro-reflector arrays. In: Bowhill SA, Jaffe LD, Rycroft MJ (eds) *Space research conference, space research conference, vol 1*. Akademie-Verlag, Berlin, pp 247–259
- Chapront J, Chapront-Touzé M, Francou G (1999) Determination of the lunar orbital and rotational parameters and of the ecliptic reference system orientation from LLR measurements and IERS data. *Astron Astrophys* 343:624–633
- Chapront J, Chapront-Touzé M, Francou G (2002) A new determination of lunar orbital parameters, precession constant and tidal acceleration from LLR measurements. *Astron Astrophys* 387:700–709. <https://doi.org/10.1051/0004-6361:20020420>

- Ciufolini I, Paolozzi A, Pavlis EC, Koenig R, Ries J, Gurzadyan V, Matzner R, Penrose R, Sindoni G, Paris C, Khachatryan H, Mirzoyan S (2016) A test of general relativity using the LARES and LAGEOS satellites and a GRACE Earth gravity model. *Eur Phys J C* 76:120. <https://doi.org/10.1140/epjc/s10052-016-3961-8>
- Colladay D, Kostelecký VA (1997) CPT violation and the standard model. *Phys Rev D* 55:6760–6774. <https://doi.org/10.1103/PhysRevD.55.6760>
- Colladay D, Kostelecký VA (1998) Lorentz-violating extension of the standard model. *Phys Rev D* 58(11):116002. <https://doi.org/10.1103/PhysRevD.58.116002>
- Combrinck L (2011) Development of a satellite and lunar laser ranger and its future applications in South Africa. In: IAC2011, October 2011, Cape Town, vol IAC-11-A2.1. <https://doi.org/10.13140/2.1.1743.3928>
- Courde C, Torre JM, Samain E, Martinot-Lagarde G, Aimar M, Albanese D, Exertier P, Fienga A, Maríe H, Metris G, Viot H, Viswanathan V (2017) Lunar laser ranging in infrared at the Grasse laser station. *Astron Astrophys* 602:A90. <https://doi.org/10.1051/0004-6361/201628590>
- Currie DG, Dell’Agnello S, Delle Monache GO, Behr B, Williams JG (2013) A lunar laser ranging retroreflector array for the 21st century. *Nucl Phys B (Proc. Suppl.)* 243:218–228. <https://doi.org/10.1016/j.nuclphysbps.2013.09.007>
- Damour T, Nordtvedt K (1993) Tensor-scalar cosmological models and their relaxation toward general relativity. *Phys Rev D* 48:3436–3450. <https://doi.org/10.1103/PhysRevD.48.3436>
- Damour T, Schäfer G (1991) New tests of the strong equivalence principle using binary-pulsar data. *Phys Rev Lett* 66:2549–2552. <https://doi.org/10.1103/PhysRevLett.66.2549>
- Damour T, Vokrouhlický D (1996) Equivalence principle and the Moon. *Phys Rev D* 53:4177–4201. <https://doi.org/10.1103/PhysRevD.53.4177>
- Degnan JJ (2008) Laser Transponders for High-Accuracy Interplanetary Laser Ranging and Time Transfer. In: Dittus H, Lämmerzahl C, Turyshev SG (ed) *Lasers, clocks and drag-free control: exploration of relativistic gravity in space, astrophysics and space science library*, vol 349, pp 231–242. https://doi.org/10.1007/978-3-540-34377-6_11
- Dickey JO, Newhall XX, Williams JG (1985) Earth orientation from lunar laser ranging and an error analysis of polar motion services. *J Geophys Res* 90:9353–9362. <https://doi.org/10.1029/JB090iB11p09353>
- Dvali G, Gabadadze G, Shifman M (2003a) Diluting the cosmological constant in infinite volume extra dimensions. *Phys Rev D* 67(4):044020. <https://doi.org/10.1103/PhysRevD.67.044020>
- Dvali G, Gruzinov A, Zaldarriaga M (2003b) The accelerated universe and the Moon. *Phys Rev D* 68(2):024012. <https://doi.org/10.1103/PhysRevD.68.024012>
- Eckhardt DH (1993) Passing through resonance: the excitation and dissipation of the lunar free libration in longitude. *Celest Mech Dyn Astron* 57:307–324. <https://doi.org/10.1007/BF00692481>
- Everitt CWF, Debra DB, Parkinson BW, Turneaure JP, Conklin JW, Heifetz MI, Keiser GM, Silbergleit AS, Holmes T, Kolodziejczak J, Al-Meshari M, Mester JC, Muhlfelder B, Solomonik VG, Stahl K, Worden PW Jr, Benzec W, Buchman S, Clarke B, Al-Jadaan A, Al-Jibreen H, Li J, Lipa JA, Lockhart JM, Al-Suwaidan B, Taber M, Wang S (2011) Gravity probe B: final results of a space experiment to test general relativity. *Phys Rev Lett* 106:221101. <https://doi.org/10.1103/PhysRevLett.106.221101>
- Faller J, Winer I, Carrion W, Johnson TS, Spadin P, Robinson L, Wampler EJ, Wieber D (1969) Laser beam directed at the lunar retro-reflector array: observations of the first returns. *Science* 166:99–102. <https://doi.org/10.1126/science.166.3901.99>
- Folkner WM, Charlot P, Fingers MH, Williams JG, Sovers OJ, Newhall XX, Standish EM (1994) Determination of the extragalactic-planetary frame tie from joint analysis of radio interferometric and lunar laser ranging measurements. *Astron Astrophys* 287:279–289
- Folkner WM, Williams JG, Boggs DH, Park RS, Kuchynka P (2014) The planetary and lunar ephemerides DE430 and DE431. *Interplanet Netw Prog Rep* 42–196:1–81
- Genova A, Mazarico E, Goossens S, Lemoine FG, Neumann GA, Smith DE, Zuber MT (2018) Solar system expansion and strong equivalence principle as seen by the NASA MESSENGER mission. *Nat Commun* 9(289):1–9. <https://doi.org/10.1038/s41467-017-02558-1>
- Grechukhin IA, Grishin EA, Ivlev OA, Kornev AF, Mak AA, Sadovnikov MA, Shargorodskiy VD (2016) Russian lunar laser locator with millimeter accuracy. 2016 International conference on laser optics (LO) R6-3, 27 June–1 July 2016, St. Petersburg, Russia. <https://doi.org/10.1109/LO.2016.7549805>
- Gross RS, Vondrák J (1999) Astrometric and space-geodetic observations of polar wander. *Geophys Res Lett* 26:2085–2088. <https://doi.org/10.1029/1999GL900422>
- Harada W, Fukushima T (2003) Harmonic decomposition of time ephemeris TE405. *Astron J* 126:2557–2561. <https://doi.org/10.1086/378909>
- Herring T (1991) The ZMOA-1990 nutation series. In: Hughes JA, Smith CA, Kaplan GH (eds) *IAU colloquium 127*, October 1990, Washington DC, USA
- Herring T, Mathews PM, Buffett BA (2002) Modeling of nutation-precession: very long baseline interferometry results. *J Geophys Res* 107(B4):2069. <https://doi.org/10.1029/2001JB000165>
- Hilton JL, Capitaine N, Chapront J, Ferrandiz JM, Fienga A, Fukushima T, Getino J, Mathews P, Simon JL, Soffel M, Vondrák J, Wallace P, Williams J (2006) Report of the international astronomical union division I working group on precession and the ecliptic. *Celest Mech Dyn Astron* 94:351–367. <https://doi.org/10.1007/s10569-006-0001-2>
- Hofmann F (2017) Lunar Laser Ranging - verbesserte Modellierung der Mondodynamik und Schätzung relativistischer Parameter. PhD thesis, Leibniz Universität Hannover, Deutsche Geodätische Kommission bei der Bayerischen Akademie der Wissenschaften, Series C 797. http://www.dgk.badw.de/fileadmin/user_upload/Files/DGK/docs/c-797.pdf
- Hofmann F, Müller J (2018) Relativistic tests with lunar laser ranging. *Class Quantum Grav* 35:035015. <https://doi.org/10.1088/1361-6382/aa8f7a>
- Hofmann F, Biskupek L, Müller J (2018) Contributions to reference systems from lunar laser ranging using the IFE analysis model. *J Geod* 92(9):975–987. <https://doi.org/10.1007/s00190-018-1109-3>
- IAU (2009) Numerical standards for fundamental astronomy: IAU2009 system of astronomical constants, XXVIIth IAU general assembly, Division 1, August 2009, Rio de Janeiro, Brazil
- Kozai Y (1972) Lunar laser ranging experiments in Japan. In: Bowhill SA, Jaffe LD, Rycroft MJ (eds) *Space research conference, space research conference*, vol 1. Akademie-Verlag, Berlin, pp 211–217
- Kopeikin SM (2010) The gravitomagnetic influence on Earth-orbiting spacecrafts and on the lunar orbit. In: Ciufolini I, Matzner RA (eds) *Astrophysics and space science library*, vol 367. Springer, Dordrecht, pp 337–343
- Kopeikin S, Xie Y (2010) Celestial reference frames and the gauge freedom in the post-Newtonian mechanics of the Earth–Moon system. *Celest Mech Dyn Astron* 108:245–263
- Kopeikin S, Pavlis E, Pavlis D, Brumberg VA, Escapa A, Getino J, Gusev A, Müller J, Ni WT, Petrova N (2008) Prospects in the orbital and rotational dynamics of the Moon with the advent of sub-centimeter lunar laser ranging. *Adv Space Res* 42(8):1378–1390. <https://doi.org/10.1016/j.asr.2008.02.014>

- Lue A, Starkman G (2003) Gravitational leakage into extra dimensions: probing dark energy using local gravity. *Phys Rev D* 67(6):064002. <https://doi.org/10.1103/PhysRevD.67.064002>
- Manche H (2011) élaboration de l'éphéméride inop: modèle dynamique et ajustements aux données de télémétrie laser lune. PhD thesis, Observatoire de Paris. <https://tel.archives-ouvertes.fr/tel-00689852>
- Mathews PM, Herring TA, Buffett BA (2002) Modeling of nutation and precession: new nutation series for nonrigid Earth and insights into the Earth's interior. *J Geophys Res (Solid Earth)* 107:2068. <https://doi.org/10.1029/2001JB000390>
- Müller J (1991) Analyse von Lasermessungen zum Mond im Rahmen einer post-Newton'schen Theorie. PhD thesis, Technische Universität München, Deutsche Geodätische Kommission bei der Bayerischen Akademie der Wissenschaften, Series C 383
- Müller J (2008) Lunar laser ranging: a space geodetic technique to test relativity. In: Kleinert H, Jantzen RT, Ruffini R (eds) The eleventh Marcel Grossmann meeting on recent developments in theoretical and experimental general relativity, gravitation and relativistic field theories, pp 2576–2578. https://doi.org/10.1142/9789812834300_0463
- Müller J, Nordtvedt K, Vokrouhlický D (1996) Improved constraint on the α_1 PPN parameter from lunar motion. *Phys Rev D* 54:5927. <https://doi.org/10.1103/PhysRevD.54.R5927>
- Müller J, Soffel M, Klioner SA (2008a) Geodesy and relativity. *J Geod* 82:133–145. <https://doi.org/10.1007/s00190-007-0168-7>
- Müller J, Williams JG, Turyshev SG (2008b) Lunar laser ranging contributions to relativity and geodesy. In: Dittus H, Lämmerzahl C, Turyshev SG (ed) Lasers, clocks and drag-free control: exploration of relativistic gravity in space, astrophysics and space science library, vol 349, pp 457–472. https://doi.org/10.1007/978-3-540-34377-6_21
- Müller J, Biskupek L, Oberst J, Schreiber U (2009) Contribution of Lunar Laser Ranging to Realise Geodetic Reference Systems. In: Drewes H, Sideris MG (eds) Geodetic reference frames, international association of geodesy symposia, vol 134. Springer, Berlin, pp 55–59. https://doi.org/10.1007/978-3-642-00860-3_8
- Müller J, Biskupek L, Hofmann F, Mai E (2014) Lunar laser ranging and relativity. In: Kopeikin S (ed) Frontiers in relativistic celestial mechanics, vol 2. de Gruyter, Berlin, pp 103–156
- Müller J, Biskupek L, Hofmann F (2015) Earth orientation and relativity parameters determined from LLR data. In: Proceedings of the 19th international workshop on laser ranging, 27–31 Oct 2014, Annapolis, MD, USA. https://cdis.nasa.gov/lw19/docs/2014/Papers/3033_Mueller_paper.pdf
- Murphy TW (2009) Lunar ranging, gravitomagnetism, and APOLLO. *Space Sci Rev* 148:217–223. <https://doi.org/10.1007/s11214-009-9491-z>
- Murphy TW (2013) Lunar laser ranging: the millimeter challenge. *Rep Prog Phys* 76(7):076901. <https://doi.org/10.1088/0034-4885/76/7/076901>
- Murphy T, Adelberger E, Battat J, Hoyle C, Michelsen E, Stubbs C, Swanson H (2006) APOLLO springs to life: one-millimeter LLR. In: Proceedings of the 15th international workshop on laser ranging, 15–20 Oct 2006, Canberra, Australia, vol 2, pp 540–545
- Murphy TW, Nordtvedt K, Turyshev S (2007) Gravitomagnetic influence on gyroscopes and on the lunar orbit. *Phys Rev Lett* 98(7):071102. <https://doi.org/10.1103/PhysRevLett.98.071102>
- Murphy T, Adelberger E, Battat J, Hoyle C, McMillan R, Michelsen E, Stubbs C, Swanson H (2008a) APOLLO: two years of science data. In: Proceedings of the 16th international workshop on laser ranging, 12–17 Oct 2008, Poznan, Poland, vol 1, pp 264–269
- Murphy TW, Adelberger EG, Battat JBR, Carey LN, Hoyle CD, Leblanc P, Michelsen EL, Nordtvedt K, Orin AE, Strasburg JD, Stubbs CW, Swanson HE, Williams E (2008b) The Apache point observatory lunar laser-ranging operation: instrument description and first detections. *Publ Astron Soc Pac* 120:20–37. <https://doi.org/10.1086/526428>
- Murphy TW, Adelberger EG, Battat JBR, Hoyle CD, McMillan RJ, Michelsen EL, Samad RL, Stubbs CW, Swanson HE (2010) Long-term degradation of optical devices on the Moon. *Icarus* 208:31–35. <https://doi.org/10.1016/j.icarus.2010.02.015>
- Murphy TW, Adelberger EG, Battat JBR, Hoyle CD, Johnson NH, McMillan RJ, Michelsen EL, Stubbs CW, Swanson HE (2011) Laser ranging to the lost Lunokhod 1 reflector. *Icarus* 211:1103–1108. <https://doi.org/10.1016/j.icarus.2010.11.010>
- Newhall XX, Williams JG (1997) Estimation of the lunar physical librations. *Celest Mech Dyn Astron* 66:21–30
- Nordtvedt K (1968a) Equivalence principle for massive bodies I. *Phenomenol Phys Rev* 169:1014–1016. <https://doi.org/10.1103/PhysRev.169.1014>
- Nordtvedt K (1968b) Equivalence principle for massive bodies. II. *Theory Phys Rev* 169:1017–1025. <https://doi.org/10.1103/PhysRev.169.1017>
- Nordtvedt K (1968c) Testing relativity with laser ranging to the Moon. *Phys Rev* 170:1186–1187. <https://doi.org/10.1103/PhysRev.170.1186>
- Nordtvedt K (1987) Probing gravity to the second post-Newtonian order and to one part in 10^7 using the spin axis of the Sun. *Astrophys J* 320:871–874. <https://doi.org/10.1086/165603>
- Nordtvedt K (1995) The relativistic orbit observables in lunar laser ranging. *Icarus* 114:51–62. <https://doi.org/10.1006/icar.1995.1042>
- Nordtvedt K Jr, Will CM (1972) Conservation laws and preferred frames in relativistic gravity. II. Experimental evidence to rule out preferred-frame theories of gravity. *Astrophys J* 177:775. <https://doi.org/10.1086/151755>
- Orszag A, Roesch J, Calame O (1972) La station de télémétrie laser de l'observatoire du Pic-du-Midi et l'acquisition des cataphotes français de Luna 17. In: Bowhill SA, Jaffe LD, Rycroft MJ (eds) Space research conference, space research conference, vol 1, pp 205–209
- Otsubo T, Kunimori H, Noda H, Hanada H (2010) Simulation of optical response of retroreflectors for future lunar laser ranging. *Adv Space Res* 45:733–740. <https://doi.org/10.1016/j.asr.2009.12.003>
- Park RS, Folkner WM, Konopliv AS, Williams JG, Smith DE, Zuber MT (2017) Precession of Mercury's Perihelion from ranging to the MESSENGER spacecraft. *Astron J* 153:121. <https://doi.org/10.3847/1538-3881/aa5be2>
- Pavlov DA, Williams JG, Suvorkin VV (2016) Determining parameters of Moon's orbital and rotational motion from LLR observations using GRAIL and IERS-recommended models. *Celest Mech Dyn Astron* 126:61–88. <https://doi.org/10.1007/s10569-016-9712-1>
- Pearlman MR, Degnan JJ, Bosworth JM (2002) The international laser ranging service. *Adv Space Res* 30:135–143. [https://doi.org/10.1016/S0273-1177\(02\)00277-6](https://doi.org/10.1016/S0273-1177(02)00277-6)
- Petit G, Luzum B (eds) (2010) IERS conventions (2010), vol IERS technical note 36. Verlag des Bundesamtes für Kartographie und Geodäsie
- Petrova NK, Nefedyev YA, Zagidullin AA, Andreev AO (2018) Use of an analytical theory for the physical libration of the Moon to detect free nutation of the lunar core. *Astron Rep* 62:1021–1025. <https://doi.org/10.1134/S1063772918120120>
- Pitjeva EV, Pavlov DA (2017) EPM2017 and EPM2017H. <http://iaaras.ru/en/dept/ephemeris/epm/2017/>. Accessed 14 Jan 2018
- Rambaux N, Williams JG (2011) The Moon's physical librations and determination of their free modes. *Celest Mech Dyn Astron* 109:85–100. <https://doi.org/10.1007/s10569-010-9314-2>
- Ratcliff JT, Gross RS (2018) Combinations of Earth orientation measurements: SPACE2017, COMB2017, and POLE2017. JPL Publication, California, pp 5–18
- Samain E, Abchiche A, Albanese D, Geyskens N, Buchholtz G, Drean A, Dufour J, Eysseric J, Exertier P, Pierron F, Pierron M, Mar-

- tinot L G, Paris J, Torre JM, Viot H (2008) MEO: the new French lunar laser ranging station. In: 16th International workshop on laser ranging, p 88
- Schreiber U, Müller J, Dassing R, Brandl N, Haufe KH, Herold G, Kahn R, Röttcher K, Stöger R (1992) LLR-activities in Wettzell. In: Proceedings of the 8th workshop on laser ranging, instrumentation, May 18. 22. 1992, Annapolis, USA, pp 10–14
- Shelus PJ (1985) MLRS: a lunar/artificial satellite laser ranging facility at the McDonald observatory. *IEEE Trans Geosci Remote Sens* 23:385–390. <https://doi.org/10.1109/TGRS.1985.289428>
- Shelus PJ (1987) To the Moon and back. *Discovery (Research and Scholarship)* 10(4):33–37
- Shelus PJ, Whipple AL, Wiant JR, Ricklefs RL, Melsheimer F (1993) A computer-controlled x-y offset guiding stage for the MLRS. In: NASA conference Publication, pp 3214, 101–105
- Silverberg EC (1974) Operation and performance of a lunar laser ranging station. *Appl Opt* 13:565–574. <https://doi.org/10.1364/AO.13.000565>
- Soffel M, Klioner SA, Petit G, Wolf P, Kopeikin SM, Bretagnon P, Brumberg VA, Capitaine N, Damour T, Fukushima T, Guinot B, Huang T-Y, Lindgren L, Ma C, Nordvedt K, Ries JC, Seidelmann PK, Vokrouhlický D, Will CM, Xu C (2003) The IAU 2000 resolutions for astrometry, celestial mechanics, and metrology in the relativistic framework: explanatory supplement. *Astron J* 126:2687–2706. <https://doi.org/10.1086/378162>
- Soffel M, Klioner S, Müller J, Biskupek L (2008) Gravitomagnetism and lunar laser ranging. *Phys Rev D* 78(2):024033. <https://doi.org/10.1103/PhysRevD.78.024033>
- Standish EM Jr (1981) Two differing definitions of the dynamical equinox and the mean obliquity. *Astron Astrophys* 101:L17
- Standish EM, Williams JG (2012) Orbital ephemerides of the Sun, Moon, and Planets, Chap. 8. In: Seidelmann PK (ed) Explanatory supplement to the astronomical almanac. U.S. Naval Observatory, Washington, D.C
- Steinhardt PJ, Wesley D (2010) Exploring extra dimensions through observational tests of dark energy and varying Newton's constant. [arXiv:1003.2815](https://arxiv.org/abs/1003.2815)
- Thorne KS, Hartle JB (1985) Laws of motion and precession for black holes and other bodies. *Phys Rev D* 31:1815–1837. <https://doi.org/10.1103/PhysRevD.31.1815>
- Turyshv SG, Williams JG (2007) Space-based tests of gravity with laser ranging. *Int J Mod Phys D* 16:2165–2179. <https://doi.org/10.1142/S0218271807011838>
- Turyshv SG, Williams JG, Folkner WM, Gutt GM, Baran RT, Hein RC, Somawardhana RP, Lipa JA, Wang S (2013) Corner-cube retro-reflector instrument for advanced lunar laser ranging. *Exp Astron* 36:105–135. <https://doi.org/10.1007/s10686-012-9324-z>
- Vasilyev MV, Yagudina EI, Grishin EA, Ivlev OA, Grechukhin IA (2016) On the accuracy of lunar ephemerides using the data provided by the future Russian lunar laser ranging system. *Sol Syst Res* 50:361–367. <https://doi.org/10.1134/S0038094616050075>
- Veillet C (1987) La distance Terre-Lune à quelques centimètres près. *La Recherche* 18:394
- Veillet C, Mangin JF, Chabaudie JE, Dumolin C, Feraudy D, Torre JM (1993) Lunar laser ranging at CERGA for the ruby period (1981–1986). *American Geophysical Union, Washington*, pp 189–193. <https://doi.org/10.1029/GD025p0189>
- Viswanathan V, Fienga A, Gastineau M, Laskar J (2017) INPOP17a planetary ephemerides. *Notes Scientifiques et Techniques de l'Institut de Mécanique Céleste, Paris*
- Viswanathan V, Fienga A, Minazzoli O, Bernus L, Laskar J, Gastineau M (2018) The new lunar ephemeris INPOP17a and its application to fundamental physics. *Mon Not R Astron Soc.* <https://doi.org/10.1093/mnras/sty096>
- Vokrouhlický D (1997) A note on the solar radiation perturbations of lunar motion. *Icarus* 126:293–300. <https://doi.org/10.1006/icar.1996.5652>
- Will CM (1993) Theory and experiment in gravitational physics. Cambridge University Press, Cambridge
- Will CM (2014) The confrontation between general relativity and experiment. *Living Rev Relat* 17(4):4. [10.12942/lrr-2014-4](https://doi.org/10.12942/lrr-2014-4)
- Williams JG (1994) Contributions to the Earth's obliquity rate, precession, and nutation. *Astron J* 108(2):711–724. <https://doi.org/10.1086/117108>
- Williams JG (2007) A scheme for lunar inner core detection. *Geophys Res Lett* 34:3202
- Williams JG, Boggs DH (2009) Lunar core and mantle. What does LLR see? In: Schillak S (ed) Proceedings of the 16th international workshop on laser ranging 1:101–120, 13.-17.08.2008, Poznań, Poland
- Williams JG, Boggs DH (2015) Tides on the Moon: theory and determination of dissipation. *J Geophys Res (Planets)* 120:689–724. <https://doi.org/10.1002/2014JE004755>
- Williams JG, Boggs DH (2016) Secular tidal changes in lunar orbit and Earth rotation. *Celest Mech Dyn Astron* 126:89–129. <https://doi.org/10.1007/s10569-016-9702-3>
- Williams JG, Folkner WM (2009) Lunar laser ranging: relativistic model and tests of gravitational physics. In: IAU symposium #261. American Astronomical Society, vol 261, p 882
- Williams JG, Newhall XX, Dickey JO (1996a) Lunar moments, tides, orientation and coordinate frames. *Planet Space Sci* 44:1077–1080
- Williams JG, Newhall XX, Dickey JO (1996b) Relativity parameters determined from lunar laser ranging. *Phys Rev D* 53:6730–6739. <https://doi.org/10.1103/PhysRevD.53.6730>
- Williams JG, Boggs DH, Yoder CF, Ratcliff JT, Dickey JO (2001) Lunar rotational dissipation in solid body and molten core. *J Geophys Res (Planets)* 106:27933–27968
- Williams JG, Turyshv SG, Boggs DH, Ratcliff JT (2006) Lunar laser ranging science: gravitational physics and lunar interior and geodesy. *Adv Space Res* 37(1):67–71. <https://doi.org/10.1016/j.asr.2005.05.013>
- Williams JG, Turyshv SG, Boggs DH (2009) Lunar laser ranging tests of the equivalence principle with the Earth and Moon. *Int J Mod Phys D* 18:1129–1175. <https://doi.org/10.1142/S021827180901500X>
- Williams JG, Turyshv SG, Boggs DH (2012) Lunar laser ranging tests of the equivalence principle. *Class Quantum Grav* 29(18):184004
- Williams JG, Boggs DH, Folkner WM (2013) DE430 lunar orbit, physical librations and surface coordinates. Technical Report IOM 335-JW,DB,WF-20130722-016, Jet Propulsion Laboratory
- Williams JG, Konopliv AS, Boggs DH, Park RS, Yuan DN, Lemoine FG, Goossens S, Mazarico E, Nimmo F, Weber RC, Asmar SW, Melosh HJ, Neumann GA, Phillips RJ, Smith DE, Solomon SC, Watkins MM, Wieczorek MA, Andrews-Hanna JC, Head JW, Kiefer WS, Matsuyama I, McGovern PJ, Taylor GJ, Zuber MT (2014) Lunar interior properties from the GRAIL mission. *J Geophys Res (Planets)* 119(7):1546–1578. <https://doi.org/10.1002/2013JE004559>
- Yang YZ, Li JL, Ping JS, Hanada H (2017) Determination of the free lunar libration modes from ephemeris DE430. *Res Astron Astrophys* 17:127. <https://doi.org/10.1088/1674-4527/17/12/127>
- Yoder CF (1981) The free librations of a dissipative Moon. *Philos Trans R Soc Lond A* 303:327–338. <https://doi.org/10.1098/rsta.1981.0206>
- Yoder CF (1995) Venus' free obliquity. *Icarus* 117:250–286. <https://doi.org/10.1006/icar.1995.1156>
- Zerhouni W, Capitaine N (2009) Celestial pole offsets from lunar laser ranging and comparison with VLBI. *Astron Astrophys* 507:1687–1695. <https://doi.org/10.1051/0004-6361/200912644>